



HAL
open science

Holocene glacier culminations in the Western Alps and their hemispheric relevance

Irene Schimmelpfennig, J.M. Schaefer, N. Akçar, S. Ivy-Ochs, R. C. Finkel, C. Schlüchter

► **To cite this version:**

Irene Schimmelpfennig, J.M. Schaefer, N. Akçar, S. Ivy-Ochs, R. C. Finkel, et al.. Holocene glacier culminations in the Western Alps and their hemispheric relevance. *Geology*, 2012, 40 (10), pp.891-894. 10.1130/G33169.1 . hal-01680367

HAL Id: hal-01680367

<https://hal.science/hal-01680367>

Submitted on 1 May 2019

HAL is a multi-disciplinary open access archive for the deposit and dissemination of scientific research documents, whether they are published or not. The documents may come from teaching and research institutions in France or abroad, or from public or private research centers.

L'archive ouverte pluridisciplinaire **HAL**, est destinée au dépôt et à la diffusion de documents scientifiques de niveau recherche, publiés ou non, émanant des établissements d'enseignement et de recherche français ou étrangers, des laboratoires publics ou privés.

1 Holocene glacier culminations in the Western Alps and their 2 hemispheric relevance

3 I. Schimmelpfennig¹, J.M. Schaefer^{1,2}, N. Akçar³, S. Ivy-Ochs⁴, R.C. Finkel⁵, and C.
4 Schlüchter³

5 ¹*Lamont-Doherty Earth Observatory, Palisades, NY, USA*

6 ²*Department of Earth and Environmental Sciences, Columbia University, New York, NY, USA*

7 ³*Institute of Geological Sciences, University of Bern, Switzerland*

8 ⁴*Institut für Teilchenphysik, Eidgenössische Technische Hochschule Zürich, Switzerland*

9 ⁵*Earth and Planetary Science Department, University of California–Berkeley, CA, USA*

10 ABSTRACT

11 The natural variability of Holocene climate defines the baseline to assess ongoing climate
12 change. Greenland ice-core records indicate warming superimposed by abrupt climate
13 oscillations in the early Holocene, followed by a general cooling trend throughout the mid- and
14 late Holocene that culminated during the Little Ice Age (LIA). Tropical precipitation changes
15 correlate with these patterns throughout the Holocene.

16 Here we use mountain glaciers in the Alps to reconstruct the regional Holocene climate
17 evolution and to test for a link between mid-latitude, North Atlantic and tropical climate. Our
18 precise ¹⁰Be chronology from Tsidjiore Nouve Glacier, western Swiss Alps, indicates a glacier
19 culmination during the earliest Holocene ~11.4 k.y. ago, likely related to the Preboreal
20 Oscillation. Based on our data, no Holocene glacier advance of similar amplitude occurred until
21 ~3.8 k.y. ago, when the glacier reached LIA limits. ¹⁰Be ages between 500 and 170 yr
22 correspond to the LIA, while the youngest ¹⁰Be ages overlap with the historically recorded post-

23 LIA glacier positions. Integrating our data with existing records, we propose a hemispheric
24 climate link between the Alps, North Atlantic temperature and tropical precipitation patterns for
25 the Holocene, supporting the concept of a pervasive climate driver. These findings from northern
26 mid-latitudes are consistent with the hypothesis formulated for the tropics that the earth's thermal
27 equator, responding to North Atlantic temperature changes, might have migrated southward
28 throughout the Holocene, reaching the southern turning point towards the end of the LIA.

29 INTRODUCTION

30 While there is increasing evidence that the climate during the current warm period, the
31 Holocene, has been less stable than originally thought (e.g., Haug et al., 2001), robust terrestrial
32 data quantifying Holocene climate changes remain sparse mostly due to their moderate
33 amplitude compared to the dramatic climate fluctuations during ice-ages. The Greenland
34 temperature record indicates rapid warming after the Younger Dryas (YD, ~12,900–11,700 years
35 ago), interrupted by early Holocene abrupt cold events such as the Preboreal Oscillation (PBO;
36 Rasmussen et al., 2007). Warm early Holocene conditions in the North Atlantic area are
37 followed by a long-term cooling (Cuffey and Clow, 1997), culminating in the Little Ice Age
38 (LIA, 1300–1850 common era, CE, e.g. Holzhauser et al., 2005). Hydrological changes in the
39 tropics correlate with long- and short-term climate events in the North Atlantic (Haug et al.,
40 2001; Sachs et al., 2009), implying shifts in the Intertropical Convergence Zone (ITCZ) as a
41 result of the thermal equator adjusting to northern temperature changes. If this scenario is
42 correct, the mid-latitudes should have responded to polar cold and warm spells, but evidence
43 remains controversial.

44 Here we use glacier fluctuations in the Western Alps to reconstruct regional Holocene
45 climate patterns and to test the link between polar climate changes and mid-latitude mountain

46 glaciers, which are highly sensitive to regional climate changes and in particular, to summer
47 temperature variations (Oerlemans, 2005). We produced a detailed moraine map and a precise
48 ^{10}Be chronology for one of the best resolved Holocene lateral moraine sequences in the Alps
49 (Fig. 1); it was deposited by the Tsidjiore Nouve Glacier in the Valais, Switzerland, one of the
50 most climate sensitive glaciers in the Swiss Alps (Röthlisberger, 1976). The overall goal of this
51 study is to test for glacier fluctuations related to the early Holocene abrupt climate changes and
52 to add constraints of climate's evolution during the mid- and late Holocene, including the LIA
53 period. In the Alps, Holocene moraine chronologies are scarce (Joerin et al., 2006), as the LIA
54 advances wiped out the older moraines in most places (Röthlisberger and Schneebeli, 1979). A
55 few pioneering surface exposure dating studies from the Swiss and Austrian Alps (Ivy-Ochs et
56 al., 2009; Schindelwig et al., 2011) report glacier advances exceeding the LIA position during
57 the early Holocene, and correlate those advances to North Atlantic cold pulses.

58 GEOMORPHIC SETTING

59 The well-preserved sequence of Holocene lateral moraine ridges at Tsidjiore Nouve
60 Glacier (Fig. 1) is composed of i) an outermost *pre-LIA moraine*: an up to 20 m high and 1 km
61 long well-defined moraine ridge. At least five recessional sub-ridges, less than 1 m high, line its
62 ice-proximal flank. Large boulders are embedded on all ridges; ii) a '*LIA*' *composite moraine*:
63 An up to 60 m high and 3 km long moraine wall, formed by at least five sub-ridges with few
64 boulders. Such massive composite moraines fringing the non-vegetated glacier forefield are
65 typically referred to as '*LIA*' moraines in the Alps (Röthlisberger and Schneebeli, 1979); iii) an
66 *outer* and an *inner post-LIA moraine* inside of the '*LIA*' composite moraine with several
67 embedded boulders. These two moraines are assigned to 1920 CE and 1991 CE, respectively

68 (Abbühl et al., 2009; Fig. 1), based on direct measurements of the glacier length changes of
69 numerous glaciers in this region (Glaciological reports, 1881–2009, Fig. DR1).

70 METHODS

71 We collected 29 surface samples from large boulders protruding >0.80 m from the lateral
72 moraine ridges of Tsidjiore Nouve Glacier (Figs. 1 and DR2). All samples were processed for
73 ^{10}Be measurements at the Lamont-Doherty Earth Observatory Cosmogenic Nuclide Laboratory
74 (method in Schaefer et al., 2009; <http://www.ldeo.columbia.edu/cosmo/>). $^{10}\text{Be}/^9\text{Be}$ ratios were
75 measured at the Center for Accelerator Mass Spectrometry, Lawrence Livermore National
76 Laboratory. To calculate the surface exposure ages, we used the ^{10}Be production rate calibrated
77 in northeastern North America (Balco et al., 2009), whose value is confirmed by several recent
78 calibration experiments elsewhere in the Northern Hemisphere (e.g., Fenton et al., 2011, Briner
79 et al., 2012). ^{10}Be ages are reported in years before 2010 CE.

80 RESULTS

81 The ^{10}Be chronology at Tsidjiore Nouve is shown in Figure 1 and Table DR1. Ages from
82 the pre-LIA moraine crest ($n = 10$) range from 10.9 to 11.9 k.y. with an arithmetic mean and
83 standard deviation of 11.4 ± 0.4 k.y. (*± 0.7 k.y. including the production rate uncertainty for*
84 *comparison with other climate proxies*, shown in italic below; Fig. 2). Ages from the recessional
85 ridges of the pre-LIA moraine ($n = 7$) are between 10.9 and 11.5 k.y., and the arithmetic mean is
86 11.2 ± 0.2 k.y. (*± 0.6 k.y.*; Fig. 2). The error-weighted mean ages, 11.44 ± 0.06 k.y. for the crest
87 and 11.25 ± 0.08 k.y. for the recessional ridges are consistent with the stratigraphy.

88 The ages from the ‘LIA’ composite moraine can be divided into two groups. (i) Three
89 ages in the central part of the outmost crest are 3790 ± 200 (ARO-12), 3320 ± 170 (ARO-13) and
90 3200 ± 180 (ARO-11) years (Fig. 1). The oldest boulder protrudes from the ice-distal side of this

91 ridge, and the two younger boulders from the ice-proximal side (Fig. DR3), yielding an
92 arithmetic mean of 3260 ± 180 years. (ii) We obtain ages of 480 ± 30 (ARO-10) and 180 ± 10
93 years (ARO-9) for boulders on an inner crest; ARO-9 is from a more ice-proximal area than
94 boulder ARO-10 (Fig. DR3). On the lowest-elevation segment of the composite moraine, in a
95 stratigraphically similar position as ARO-10, sample ARO-23 yields an age of 580 ± 30 years.

96 The five samples from the outer post-LIA moraine yield ages of 170 ± 10 years (ARO-
97 66), 150 ± 10 years (ARO-67), 150 ± 10 (ARO-63), 110 ± 10 years (ARO-65) and 100 ± 10
98 years (ARO-64). One sample from the inner post-LIA moraine yields an age of 120 ± 10 years
99 (ARO-62).

100 DISCUSSION

101 The glacier chronology at Tsidjore Nouve yields constraints for five periods of Holocene
102 glacier fluctuations (Fig. 3A), which we compare to other terrestrial records in the northern mid-
103 latitudes, and to North Atlantic temperature and tropical precipitation records (Fig. 3):

104 (i) Earliest Holocene: The mean age of the pre-LIA moraine crest of ~ 11.4 k.y. indicates that the
105 Tsidjore Nouve Glacier was close to its LIA-limits at or shortly after the YD/earliest
106 Holocene transition. The mean age of the recessional ridges is slightly younger (~ 11.2 k.y.)
107 indicating that the glacier might have retreated slowly from the crest over a few centuries.

108 The age range for this moraine overlaps with both the late YD and the PBO (Fig. 3A), a brief
109 cold-spell identified in the Greenland ice cores, peaking 11.40 k.y. ago and terminating 11.27
110 k.y. ago (Rasmussen et al., 2007; Kobashi et al., 2008; Fig. 3G). Chronologically, two
111 scenarios are possible: Either the pre-LIA moraine corresponds to a late YD position of the
112 glacier, followed by a slow oscillatory retreat during the PBO marked by the recessional
113 ridges; or the pre-LIA moraine was deposited during the PBO, interrupting the glacier retreat

114 from the more extensive late glacial position. Traditionally, the YD has been related to the
115 ‘Egesen Stadial’ in the Alps (Ivy-Ochs et al., 2009, and references herein) with Egesen
116 snowlines in the region of Tsidjiore Nouve Glacier (Valais) being ~200 m below the LIA
117 maximum (Maisch, 1987), far downstream of the pre-LIA moraine. Adopting this scenario
118 here, it appears more likely that the pre-LIA moraine is related to the PBO. Independent
119 evidence in the Alps further supports the PBO signature (Fig. 3): Burga (1987) reports an
120 increase in non-arboreal pollen during the earliest Holocene in a peat bog at Palü Glacier
121 (Eastern Swiss Alps) and infers a glacier advance beyond its LIA extent (“Palü Oscillation”).
122 $\delta^{18}\text{O}$ changes in Swiss lake sediments showing a strong similarity with the Greenland $\delta^{18}\text{O}$
123 record reveal a distinct, ‘PBO-type’ signal shortly after the YD termination (Schwander et
124 al., 2000, Fig. 3F). Further evidence for the PBO in European and North American lacustrine
125 and glacial records (e.g., Björck et al., 1997; Hu et al., 2006) suggest a wide geographic
126 footprint of this short cold spell.

127 (ii) Early and mid-Holocene: It is characteristic for the Alps that no moraines are preserved
128 during the early and mid-Holocene, suggesting that glaciers were smaller during this period
129 than during the LIA (Holzhauser et al., 2005). In Greenland, a warming of 4 ± 1.5 °C within
130 ~14 years is recorded at the end of the PBO (Kobashi et al., 2008). The manifestation of this
131 abrupt warming might have driven glaciers in the Alps far inside their LIA configuration,
132 where they remained during the entire mid-Holocene. Warm early to mid-Holocene climate
133 is also supported by recent studies from the European Alps: Mont Miné Glacier, a
134 neighboring glacier of Tsidjiore Nouve, was smaller than today 9 k.y. ago, before a short-
135 lived, minor advance 8.2 k.y. ago killed many trees growing up-valley of today’s glacier
136 terminus (Nicolussi and Schlüchter, 2012; Fig. 3C); Swiss glaciers were smaller than today

137 during the early and mid-Holocene, based on sub-fossil wood and peat records (Joerin et al.,
138 2006, Fig. 3D); a speleothem record implies that the Upper Grindelwald Glacier (Swiss Alps)
139 was in a quasi-continuously retracted position until 5.8 k.y., followed by a period of larger
140 glaciers (Luetscher et al., 2011, Fig. 3E). Re-advances of glaciers in the Alps during the
141 second half of the Holocene agree with the general cooling trend in Greenland (Cuffey and
142 Clow, 1997; Fig. 3H) and correlate with a precipitation decrease in the tropics (Haug et al.,
143 2001; Fig. 3I), both beginning after the thermal maximum ~7.5 k.y. ago and culminating in
144 the LIA.

145 (iii) Late Holocene: The three boulder ages from the oldest segment of the 'LIA' composite
146 moraine provide less robust age constraints, but indicate that the glacier was similar to LIA
147 size 3.8–3.2 k.y. ago. We cannot entirely exclude the possibility of ^{10}Be accumulation prior
148 to final boulder deposition. However, several arguments support the view that these three
149 ages represent the formation of this moraine segment. First, the chronology agrees with the
150 stratigraphic order. Second, the ^{14}C -dating of a larch log found in the basal till of the
151 proglacial streambed yielded an age of 3440–2770 cal yr B.P. (Table DR2), consistent with
152 the two younger ^{10}Be ages, implying an advance of the glacier at that time (Röthlisberger,
153 1976). This scenario is further supported by ^{14}C dates on two fossil soils that formed on this
154 moraine 1510–1080 cal yr B.P. (lower horizon) and 1180–800 cal yr B.P. (upper horizon;
155 Röthlisberger, 1976, Table DR2). The ^{14}C dates assign a conservative minimum age to this
156 moraine, supporting the pre-LIA ^{10}Be ages. Interestingly, both soil-dates fall within the
157 Medieval Warm Period (MWP; Fig. 3B). Other studies in the European Alps support the
158 onset of substantial glacier re-advances to 'LIA extent' ~3.8 k.y. ago. The speleothem record
159 at Upper Grindelwald Glacier implies glacier advances close to its Holocene peak extent

160 from 3.8 k.y. ago onward (Luetscher et al., 2011, Fig. 3E). Patzelt and Bortenschlager (1973)
161 define the “Löbben Oscillation” ~4.0–3.0 cal kyr ago based on ^{14}C -dates of the advance of
162 two glaciers and climatic deterioration in a pollen record in Austria. Glacier culminations at
163 that time are also documented in other regions of the Northern Hemisphere. According to
164 Menounos et al. (2009) and references therein, glaciers in western Canada reached ‘LIA-
165 extent’ by 3.5 k.y. ago, based on ^{14}C -dates from proglacial detrital and in situ wood. In
166 southeastern Alaska, ^{14}C -dates of a tree-ring series indicate a glacial expansion ~3.4–3.0 k.y.
167 ago (Wiles et al., 2011). In the tropics, the period between ~3.8 and 2.8 k.y. ago is marked by
168 centennial-scale, large-amplitude variations in precipitation, including several precipitation
169 minima similar to those during the LIA (Haug et al., 2001; Fig. 3I).

170 (iv) Little Ice Age: Lasting from about 1300-1850 CE, the LIA in the Swiss Alps showed three
171 maxima, c. 1350, 1650 and 1850 CE (Holzhauser et al., 2005). The three younger ages on the
172 inner sub-ridge of the composite moraine correspond to the years 1430 ± 32 , 1534 ± 28 , 1829
173 ± 11 CE, all within the LIA period. A drawing of Tsidjiore Nouve Glacier from 1836 CE
174 (Fig. DR4) testifies the advanced position of the glacier terminus to be more than 1 km
175 downvalley of its modern position, and is in general agreement with the boulder age
176 corresponding to 1829 ± 11 CE (ARO-9).

177 (v) Little Ice Age Termination: Our six post-LIA boulder ages correspond to the years between
178 1840 ± 13 and 1906 ± 11 CE, broadly overlapping with the historic record (Glaciological
179 reports, 1881–2009; Fig. DR1). Offsets of ~15 to 100 years between the ^{10}Be ages and the
180 historically recorded deposition years of the post-LIA moraines (Fig. 1) are probably due to a
181 small ^{10}Be signal (~300 - 2000 atoms $^{10}\text{Be g}^{-1}$) inherited from previous exposure. This result
182 underlines the potential to resolve (sub-)centennial climate events during the last millennium

183 with ^{10}Be dating of moraines, previously only reported from New Zealand (Schaefer et al.,
184 2009) and Peru (Licciardi et al., 2009).

185 CONCLUSION

186 We make the case that Holocene glacier fluctuations in the western Alps (i.e., mid-
187 latitude temperatures) are related to North Atlantic temperature changes and the tropical
188 hydrological cycle, confirming a hemispheric climate link. Our observations thus reinforce the
189 concept of a common hemispheric driving mechanism and support the scenario that the earth's
190 thermal equator and the connected westerly winds have shifted south over several millennia
191 during the Holocene in response to North Atlantic temperature changes, reaching its
192 southernmost position during the LIA (Sachs et al., 2009).

193 ACKNOWLEDGMENTS

194 We thank R. Schwartz, J. Hanley and J. Frisch for help with sample preparation, A.
195 Putnam for assistance during figure preparation, and the staff of LLNL-CAMS for the
196 excellent measurements. We acknowledge support by the CRONUS-Earth project (NSF
197 Grant EAR-0345835), by the International Balzan Foundation and the German Academic
198 Exchange Service (DAAD). This is Lamont-Doherty Earth Observatory publication 7540.
199 Comments from Jason Briner and two anonymous reviewers greatly improved this
200 manuscript.

201 REFERENCES CITED

202 Abbühl, L., Akçar, N., Strasky, S., Graf, A., Ivy-Ochs, S., and Schlüchter, C., 2009, A zero-
203 exposure time experiment on an erratic boulder: Evaluating the problem of pre-exposure in
204 Surface Exposure Dating, *Eiszeitalter und Gegenwart: Quaternary Sciences Journal*, v. 58,
205 p. 1–11.

- 206 Balco, G., Briner, J., Finkel, R.C., Rayburn, J.A., Ridge, J.C., and Schaefer, J.M., 2009, Regional
207 beryllium-10 production rate calibration for late-glacial northeastern North America:
208 Quaternary Geochronology, v. 4, p. 93–107, doi:10.1016/j.quageo.2008.09.001.
- 209 Björck, S., Rundgren, M., Ingólfsson, Ó., and Funder, S., 1997, The Preboreal oscillation around
210 the Nordic Seas: Terrestrial and lacustrine responses: Journal of Quaternary Science, v. 12,
211 p. 455–465, doi:10.1002/(SICI)1099-1417(199711/12)12:6<455::AID-JQS316>3.0.CO;2-S.
- 212 Briner, J.P., Young, N.E., Goehring, B.M., and Schaefer, J.M., 2012, Constraining Holocene
213 ¹⁰Be production rates in Greenland, Journal of Quaternary Science, v. 27, p. 2-6, doi:
214 10.1002/jqs.1562.
- 215 Burga, C.A., 1987, Gletscher- und Vegetationsgeschichte der südrätischen Alpen seit der
216 Späteiszeit (Puschlav, Livigno, Bormiese): Denkschriften der Schweizerischen
217 Naturforschenden Gesellschaft, v. 101, 162 p.
- 218 Cuffey, K., and Clow, G., 1997, Temperature, accumulation, and ice sheet elevation in central
219 Greenland through the last deglacial transition: Journal of Geophysical Research, v. 102,
220 p. 26383–26396, doi:10.1029/96JC03981.
- 221 Fenton, C.R., Hermanns, R.L., Blikra, L.H., Kubik, P.W., Bryant, C., Niedermann, S., Meixner,
222 A., and Goethals, M.M., 2011, Regional ¹⁰Be production rate calibration for the past 12 ka
223 deduced from the radiocarbon-dated Grøtlandsura and Russenes rock avalanches at 69°N,
224 Norway: Quaternary Geochronology, v. 6, p. 437–452, doi:10.1016/j.quageo.2011.04.005.
- 225 Glaciological reports, 1881–2009, “The Swiss Glaciers”, Yearbooks of the Cryospheric
226 Commission of the Swiss Academy of Sciences (SCNAT) published since 1964 by the
227 Laboratory of Hydraulics, Hydrology and Glaciology (VAW) of ETH Zürich. No 1–126.
228 (<http://glaciology.ethz.ch/swiss-glaciers/>)

- 229 Haug, G.H., Hughen, K.A., Sigman, D.M., Peterson, L.C., and Röhl, U., 2001, Southward
230 migration of the Intertropical Convergence Zone through the Holocene: *Science*, v. 293,
231 p. 1304–1308, doi:10.1126/science.1059725.
- 232 Holzhauser, H., Magny, M., and Zumbühl, H.J., 2005, Glacier and lake-level variations in west-
233 central Europe over the last 3500 years: *The Holocene*, v. 15, p. 789–801,
234 doi:10.1191/0959683605hl853ra.
- 235 Hu, F., Nelson, D., Clarke, G., Rühland, K., Huang, Y., Kaufman, D., and Smol, J., 2006, Abrupt
236 climatic events during the last glacial-interglacial transition in Alaska: *Geophysical*
237 *Research Letters*, v. 33, L18708, 5 p.
- 238 Ivy-Ochs, S., Kerschner, H., Maisch, M., Christl, M., Kubik, P.W., and Schluechter, C., 2009,
239 Latest Pleistocene and Holocene glacier variations in the European Alps: *Quaternary*
240 *Science Reviews*, v. 28, p. 2137–2149, doi:10.1016/j.quascirev.2009.03.009.
- 241 Joerin, U.E., Stocker, T.F., and Schlüchter, C., 2006, Multicentury glacier fluctuations in the
242 Swiss Alps during the Holocene: *The Holocene*, v. 16, p. 697–704,
243 doi:10.1191/0959683606hl964rp.
- 244 Kobashi, T., Severinghaus, J.P., and Barnola, J.-M., 2008, $4\pm 1.5^\circ\text{C}$ abrupt warming 11,270 yr
245 ago identified from trapped air in Greenland ice: *Earth and Planetary Science Letters*, v. 268,
246 p. 397–407, doi:10.1016/j.epsl.2008.01.032.
- 247 Licciardi, J.M., Schaefer, J.M., Taggart, J.R., and Lund, D.C., 2009, Holocene glacier
248 fluctuations in the Peruvian Andes indicate northern climate linkages. *Science*, v. 324, p.
249 1677-1679, doi: 10.1126/science.1175010.

- 250 Luetscher, M., Hoffmann, D.L., Frisia, S., and Spötl, C., 2011, Holocene glacier history from
251 alpine speleothems, Milchbach cave, Switzerland: *Earth and Planetary Science Letters*,
252 v. 302, p. 95–106, doi:10.1016/j.epsl.2010.11.042.
- 253 Maisch, M., 1987, Zur Gletschergeschichte des alpinen Spätglazials: Analyse und Interpretation
254 von Schneegrenzdaten: *Geographica Helvetica*, v. 42, p. 63–71.
- 255 Menounos, B., Osborn, G., Clague, J.J., and Luckman, B.H., 2009, Latest Pleistocene and
256 Holocene glacier fluctuations in western Canada: *Quaternary Science Reviews*, v. 28,
257 p. 2049–2074, doi:10.1016/j.quascirev.2008.10.018.
- 258 Nicolussi, K., and Schlüchter, C., 2012, The 8.2 ka event - calendar dated glacier response in the
259 Alps: *Geology* (in press).
- 260 Oerlemans, J., 2005, Extracting a Climate Signal from 169 Glacier Records: *Science*, v. 308,
261 p. 675–677, doi:10.1126/science.1107046.
- 262 Patzelt, G., and Bortenschlager, S., 1973, Die postglazialen Gletscher- und Klimaschwankungen
263 in der Venedigergruppe (Hohe Tauern, Ostalpen), *Zeitschrift für Geomorphologie N.F.*:
264 Supplementband, v. 16, p. 27–48.
- 265 Rasmussen, S.O., Vinther, B.M., Clausen, H.B., and Andersen, K.K., 2007, Early Holocene
266 climate oscillations recorded in three Greenland ice cores: *Quaternary Science Reviews*,
267 v. 26, p. 1907–1914, doi:10.1016/j.quascirev.2007.06.015.
- 268 Röthlisberger, F., 1976, Gletscher- und Klimaschwankungen im Raum Zermatt, Ferpècle und
269 Arolla: *Die Alpen*, v. 52, p. 59–152.
- 270 Röthlisberger, F., and Schneebeli, W., 1979, Genesis of lateral moraine complexes, demonstrated
271 by fossil soils and trunks: indicators of postglacial climatic fluctuations, // Schlüchter, C.,
272 ed., *Moraines and Varves*: Rotterdam, A.A. Balkema, p. 387–419.

- 273 Sachs, J.P., Sachse, D., Smittenberg, R.H., Zhang, Z., Battisti, D.S., and Golubic, S., 2009,
274 Southward movement of the Pacific intertropical convergence zone AD 1400–1850: *Nature*
275 *Geoscience*, v. 2, p. 519–525, doi:10.1038/ngeo554.
- 276 Schaefer, J., Denton, G., Kaplan, M., Putnam, A., Finkel, R., Barrell, D., Andersen, B.,
277 Schwartz, R., Mackintosh, A., Chinn, T., and Schluechter, C., 2009, High-frequency
278 Holocene glacier fluctuations in New Zealand differ from the northern signature: *Science*,
279 v. 324, p. 622–625, doi:10.1126/science.1169312.
- 280 Schindelwig, I., Akçar, N., Kubik, P.W., and Schlüchter, C., 2011, Lateglacial and early
281 Holocene dynamics of adjacent valley glaciers in the Western Swiss Alps: *Journal of*
282 *Quaternary Science*, doi:10.1002/jqs.1523.
- 283 Schwander, J., Eicher, U., and Ammann, B., 2000, Oxygen isotopes of lake marl at Gerzensee
284 and Leysin (Switzerland), covering the Younger Dryas and two minor oscillations, and their
285 correlation to the GRIP ice core: *Palaeogeography, Palaeoclimatology, Palaeoecology*,
286 v. 159, p. 203–214, doi:10.1016/S0031-0182(00)00085-7.
- 287 Stuiver, M., Grootes, P.M., and Braziunas, T.F., 1995, The GISP2 $\delta^{18}\text{O}$ climate record of the
288 past 16,500 years and the role of the sun, ocean, and volcanoes: *Quaternary Research*, v. 44,
289 p. 341–354, doi:10.1006/qres.1995.1079.
- 290 Wiles, G.C., Lawson, D.E., Lyon, E., Wiesenberg, N., and D'Arrigo, R.D., 2011, Tree-ring dates
291 on two pre-Little Ice Age advances in Glacier Bay National Park and Preserve, Alaska,
292 USA: *Quaternary Research*, v. 76, p. 190–195, doi:10.1016/j.yqres.2011.05.005.

293 FIGURES CAPTIONS

- 294 Figure 1. Map of the Holocene moraine sequence at Tsidjiore Nouve Glacier with ^{10}Be surface-
295 exposure ages (arithmetic means, 1σ uncertainties and sample names). LIA = Little Ice Age. The

296 inset shows the study area in red. Individual ages of the pre-LIA moraine are given with
297 analytical errors only; the boulder ages of the other moraines include the production rate
298 uncertainty. Yellow boxes show the moraine names as used in the main text, blue boxes show the
299 ages of historically recorded moraines (Abbühl et al., 2009). Estimates of four moraine
300 deposition ages based on ^{14}C dated fossil soils and logs (Röthlisberger, 1976, Fig. DR5D) are
301 given in dark green boxes, and the calibrated ^{14}C ages of two fossil soils are shown in light green
302 (Röthlisberger, 1976, Fig. DR5A,B). Legend: “Late Holocene” refers here to the period starting
303 4 k.y. ago, excluding LIA and post-LIA. See Fig. DR3 for zoom-in of the ‘Late Holocene/LIA’
304 complex.

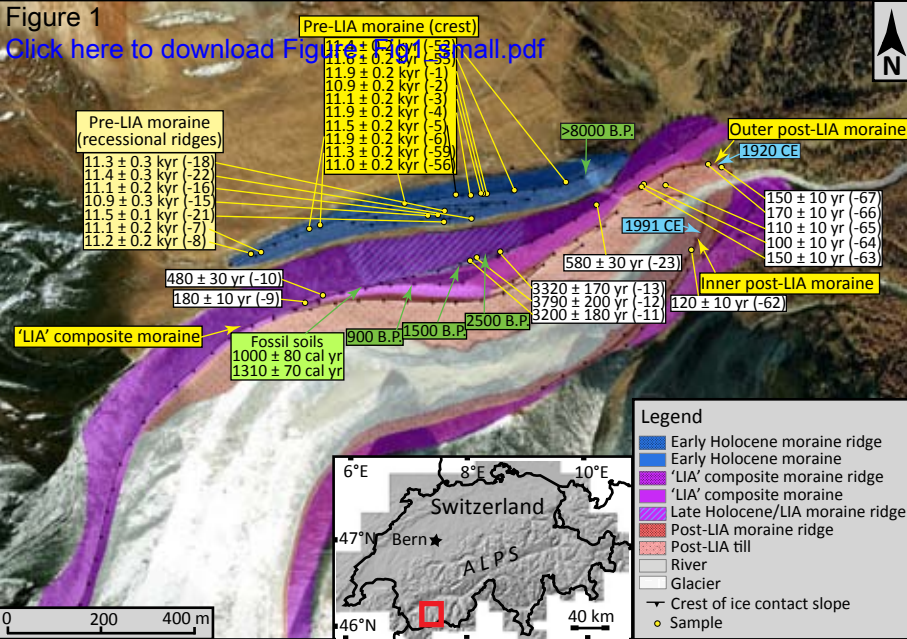
305 Figure 2. Summed probability curves of ^{10}Be ages from the crest and the recessional ridges of the
306 pre-LIA moraine ridge. Individual ages in probability plots include propagation of analytical
307 errors. The yellow bands denote the arithmetic means (= Ar. mean) and the standard deviations
308 (= st.dv.). See Table DR3 for statistics.

309 Figure 3. Comparison of Holocene climate records in the European Alps (upper panel), in
310 Greenland (middle panel) and in the tropics (lower panel). Blue generally indicates colder (in the
311 tropics dryer) and red warmer (in tropics wetter) conditions. LIA = Little Ice Age; MWP =
312 Medieval Warm Period; PBO = Preboreal Oscillation; YD = Younger Dryas. A: Holocene
313 fluctuations of Tsidjiore Nouve Glacier (46°N), represented as approximate glacier length
314 changes, estimated based on lateral moraine positions and historic records. White vertical dashed
315 lines indicate glacier length uncertainties. ^{10}Be age error bars (1σ) include the production rate
316 uncertainty. Note that moraine sequences are discontinuous records of glacier behavior, indicated
317 here by the dashed curves and the question marks. B: Two recession events of Tsidjiore Nouve
318 Glacier, evident from ^{14}C -dated soils within the ‘LIA’ composite moraine (Röthlisberger, 1976).

319 C: Re-advance of Mont Miné Glacier (Valais) to its modern extent inferred from ^{14}C -dated
320 proglacial fossil trees (Nicolussi and Schlüchter, 2012). D: Recession periods of six Swiss
321 glaciers deduced from ^{14}C -dated proglacial wood and peat (Joerin et al., 2006). E: Behavior of
322 the Upper Grindelwald Glacier inferred from petrographic and stable isotope changes in
323 speleothems (Luetscher et al., 2011). F: $\delta^{18}\text{O}$ records in sediment of two Swiss lakes at
324 Gerzensee and Leysin (Schwander et al., 2000). G: GISP2 $\delta^{18}\text{O}$ record (Stuiver et al., 1995). H:
325 500-year smoothed record of Greenland surface temperature based on GISP2 borehole
326 measurements (Cuffey and Clow, 1997). I: Titanium concentrations in Cariaco Basin sediments
327 (10°N) as a proxy for precipitation changes (Haug et al., 2001).
328 1 GSA Data Repository item 2012xxx, supporting data tables and figures, is available online at
329 www.geosociety.org/pubs/ft2012.htm, or on request from editing@geosociety.org or Documents
330 Secretary, GSA, P.O. Box 9140, Boulder, CO 80301, USA.

Figure 1

[Click here to download Figure Fig1_small.pdf](#)



Pre-LIA moraine (crest)

11.6 ± 0.2 kyr (-53)
11.6 ± 0.2 kyr (-53)
11.9 ± 0.2 kyr (-1)
10.9 ± 0.2 kyr (-2)
11.1 ± 0.2 kyr (-3)
11.9 ± 0.2 kyr (-4)
11.5 ± 0.2 kyr (-5)
11.9 ± 0.2 kyr (-6)
11.3 ± 0.2 kyr (-59)
11.0 ± 0.2 kyr (-56)

Pre-LIA moraine (recessional ridges)

11.3 ± 0.3 kyr (-18)
11.4 ± 0.3 kyr (-22)
11.1 ± 0.2 kyr (-16)
10.9 ± 0.3 kyr (-15)
11.5 ± 0.1 kyr (-21)
11.1 ± 0.2 kyr (-7)
11.2 ± 0.2 kyr (-8)

Outer post-LIA moraine

1920 CE

150 ± 10 yr (-67)
170 ± 10 yr (-66)
110 ± 10 yr (-65)
100 ± 10 yr (-64)
150 ± 10 yr (-63)

1991 CE

580 ± 30 yr (-23)

Inner post-LIA moraine

120 ± 10 yr (-62)

3320 ± 170 yr (-13)
3790 ± 200 yr (-12)
3200 ± 180 yr (-11)

'LIA' composite moraine

Fossil soils
1000 ± 80 cal yr
1310 ± 70 cal yr

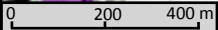
900 B.P.

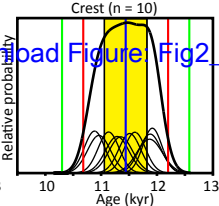
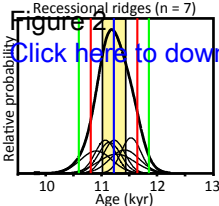
1500 B.P.

2500 B.P.

Legend

- Early Holocene moraine ridge
- Early Holocene moraine
- 'LIA' composite moraine ridge
- 'LIA' composite moraine
- Late Holocene/LIA moraine ridge
- Post-LIA moraine ridge
- Post-LIA till
- River
- Glacier
- Crest of ice contact slope
- Sample

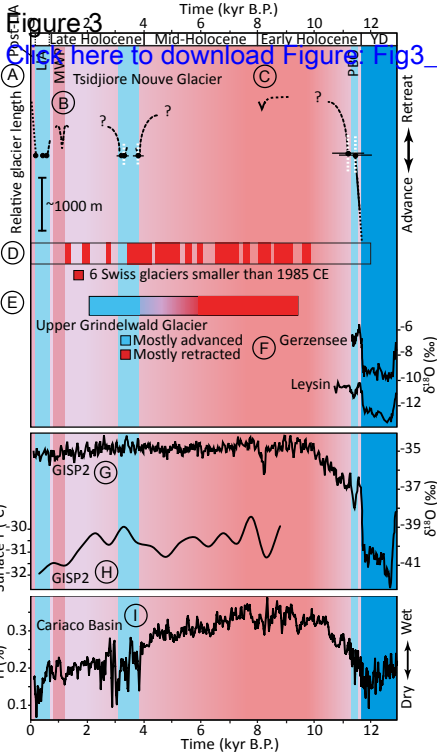




Ar. mean \pm st.dv.: 11,230 \pm 210 yr
 Weighted mean: 11,250 \pm 80 yr

Ar. mean \pm st.dv.: 11,440 \pm 380 yr
 Weighted mean: 11,440 \pm 60 yr

Figure 2
[Click here to download Figure: Fig2](#)



DATA REPOSITORY for:

**Holocene glacier culminations in the Western Alps and their
hemispheric relevance**

Irene Schimmelpfennig, Joerg M. Schaefer, Naki Akçar, Susan Ivy-Ochs, Robert C. Finkel, Christian Schlüchter

Geology

Table DR1: Sample details, analytical data and surface exposure ages. Sample $^{10}\text{Be}/^9\text{Be}$ ratios, measured at the Center for Accelerator Mass Spectrometry of the Lawrence Livermore National Laboratory, were normalized to one of the indicated standards, KNSTD (until mid-2007; $^{10}\text{Be}/^9\text{Be} = 3.15 \times 10^{-12}$) or KNSTD07 (after the year 2007; $^{10}\text{Be}/^9\text{Be} = 2.85 \times 10^{-12}$). Measurements normalized to KNSTD were corrected by a factor of 0.9048 during age calculation. The ages are calculated using the ^{10}Be production rate with a value of 3.85 ± 0.19 atoms $(\text{g yr})^{-1}$ (Balco et al. 2009, normalized to standard 07KNSTD) and the scaling method ‘Lm’ (time-dependent version of Lal, 1991) according to Balco et al. (2008). They are reported in calendar years before 2010 CE. 1σ analytical uncertainties range between 1.5% and 3%, except for samples younger than 500 years, which have uncertainties between 3% and 10%.

Sample name	Latitude (°N)	Longitude (°E)	Elevation (m)	Thickness (cm)	Shielding factor	Qtz weight (g)	Carrier (mg ^9Be)	Carrier (mg ^9Be)	$^{10}\text{Be}/^9\text{Be}$ Standard used	$^{10}\text{Be}/^9\text{Be} \times 10^{14}$	^{10}Be (x 10^3 atoms g^{-1})	^{10}Be age (years)	1σ Analyt. error	1σ error incl. prod. rate error
Pre-LIA MORaine, BOULDERS ON CREST														
ARO-4	46.01820	7.46480	2393	2.30	0.977	9.97	0.2040	BE23706	KNSTD	25.15±0.36	332.9±4.8	11920	170	610
ARO-1	46.01824	7.46527	2387	4.36	0.977	16.55	0.2077	BE23715	KNSTD	39.93±0.66	325.1±5.4	11880	200	620
ARO-6	46.01746	7.45986	2433	2.04	0.970	21.33	0.2060	BE23716	KNSTD	54.0±1.0	338.6±6.5	11870	230	630
ARO-55	46.01838	7.46628	2371	1.89	0.977	12.04	0.1829	BE31219	07KNSTD	28.59±0.46	289.9±4.7	11610	190	600
ARO-5	46.01823	7.46434	2400	3.19	0.977	10.60	0.1991	BE23707	KNSTD	26.45±0.44	321.4±5.4	11510	200	600
ARO-52	46.01858	7.46791	2345	1.91	0.978	17.54	0.1830	BE31211	07KNSTD	40.09±0.75	279.0±5.2	11350	210	600
ARO-59	46.01752	7.4602	2432	1.43	0.970	20.08	0.1836	BE31213	07KNSTD	48.04±0.89	293.1±5.5	11290	210	600
ARO-3	46.01823	7.46509	2389	2.50	0.977	10.06	0.2043	BE23705	KNSTD	23.59±0.39	309.9±5.2	11140	190	580
ARO-56	46.01798	7.46267	2419	3.27	0.974	20.08	0.1840	BE31212	07KNSTD	45.83±0.85	279.4±5.2	10960	200	580
ARO-2	46.01824	7.46516	2389	3.31	0.977	10.07	0.2050	BE23704	KNSTD	22.85±0.38	300.9±5.1	10880	180	570
Pre-LIA MORaine, BOULDERS ON RECESSONAL RIDGES														
ARO-21_2010Apr	46.01762	7.46405	2393	2.13	0.943	5.57	0.1868	BE29530	07KNSTD	12.90±0.31	285.6±7.0	11650	290	640
ARO-21	46.01762	7.46405	2393	2.13	0.943	42.19	0.2053	BE24922	07KNSTD	89.6±1.8	283.1±5.7	11630	240	620
ARO-22	46.01762	7.46477	2381	2.62	0.954	5.34	0.1894	BE28931	07KNSTD	12.23±0.28	279.2±6.6	11420	270	630
ARO-21_re	46.01762	7.46405	2393	2.13	0.943	20.15	0.1839	BE31210	07KNSTD	45.49±0.85	277.0±5.2	11330	210	600
ARO-18	46.01788	7.46407	2399	1.91	0.966	4.53	0.1878	BE28930	07KNSTD	10.66±0.30	283.8±8.2	11280	330	650
ARO-8	46.01692	7.45804	2442	3.93	0.970	10.14	0.2051	BE23708	KNSTD	24.33±0.41	318.4±5.4	11230	190	590
ARO-16	46.01777	7.46387	2399	1.61	0.954	5.14	0.1860	BE28929	07KNSTD	11.92±0.21	277.7±5.1	11150	200	590
ARO-7	46.01696	7.45834	2441	2.50	0.970	30.37	0.2048	BE23717	KNSTD	72.5±1.2	317.4±5.4	11070	190	580
ARO-15	46.01773	7.46347	2404	1.63	0.954	3.66	0.1894	BE28928	07KNSTD	8.23±0.21	273.1±7.0	10910	280	610
‘LIA’ COMPOSITE MORaine, OUTMOST SUB-RIDGE														
ARO-12	46.01678	7.46504	2416	3.24	0.981	30.05	0.2017	BE23712	KNSTD	24.49±0.41	106.4±1.8	3786	63	200
ARO-13	46.01694	7.46577	2398	2.26	0.974	30.32	0.2041	BE23713	KNSTD	21.05±0.35	91.6±1.5	3320	55	170
ARO-11	46.01675	7.46498	2419	3.79	0.981	20.80	0.1820	BE23711	KNSTD	15.78±0.39	89.0±2.2	3201	79	180
‘LIA’ COMPOSITE MORaine, LIA SUB-RIDGE														
ARO-23	46.01815	7.4691	2308	2.84	0.948	47.03	0.1535	BE26085	07KNSTD	6.34±0.14	12.92±0.33	577	15	32
ARO-10	46.01598	7.46050	2475	1.83	0.988	30.48	0.2039	BE23710	KNSTD	3.27±0.11	13.71±0.48	475	16	28
ARO-9	46.01582	7.45993	2478	2.68	0.988	30.27	0.2037	BE23709	KNSTD	1.289±0.069	5.12±0.31	181	11	14
OUTER Post-LIA RECESSONAL MORaine														
ARO-66	46.01923	7.47315	2175	3.26	0.970	28.46	0.1558	BE32368	07KNSTD	0.998±0.058	3.55±0.22	170	10	13
ARO-63	46.0186	7.47057	2255	1.61	0.970	45.39	0.1553	BE32367	07KNSTD	1.470±0.064	3.30±0.15	148	7	10
ARO-67	46.01921	7.47357	2163	3.48	0.970	38.11	0.1563	BE32369	07KNSTD	1.145±0.067	3.06±0.19	148	9	12
ARO-65	46.01923	7.47315	2222	2.41	0.958	19.96	0.1846	BE31215	07KNSTD	0.453±0.029	2.38±0.20	111	9	11
ARO-64	46.01863	7.47058	2254	1.23	0.974	19.96	0.1842	BE31214	07KNSTD	0.447±0.031	2.33±0.21	104	10	11
INNER Post-LIA RECESSONAL MORaine														
ARO-62	46.01702	7.47225	2254	2.93	0.960	49.40	0.1248	BE32366	07KNSTD	1.532±0.072	2.53±0.12	116	6	8
Blank name	Processed with						Carrier (mg ^9Be)	Carrier (mg ^9Be)	$^{10}\text{Be}/^9\text{Be}$ Standard used	$^{10}\text{Be}/^9\text{Be} \times 10^{14}$	Total number of atoms $^{10}\text{Be} \times 10^3$			
Blank_1_07Feb23	ARO-2,-3,-4,-5,-8						0.2035	BE23703	KNSTD	0.117±0.021	15.4±2.7			
Blank_2_07Feb23	ARO-9,-10,-11,-12,-13						0.2051	BE23714	KNSTD	0.118±0.019	15.8±2.5			
Blank_2_07Jan19	ARO-1,-6,-7						0.2065	BE23718	KNSTD	0.073±0.017	9.8±2.3			
Blank_1_2010Jan22	ARO-15,-16,-18,-22						0.1895	BE28932	07KNSTD	0.116±0.021	14.3±2.5			
Blank_3_08Oct06	ARO-23						0.1534	BE26086	07KNSTD	0.252±0.053	25.1±5.3			
Blank_4_07Dec05	ARO-21						0.2066	BE24923	07KNSTD	0.747±0.013	10.0±1.8			
Blank_1_2010Apr20	ARO-21						0.1868	BE29537	07KNSTD	0.150±0.023	18.7±2.8			
Blank_2_2011Jan18	2010Apr													
	ARO-21_re,-52,-56,-59,-64,-65						0.1837	BE31218	07KNSTD	0.069±0.015	8.5±1.8			
Blank_1_2011Jan18	ARO-55						0.1849	BE31221	07KNSTD	0.030±0.010	3.7±1.2			
Blank_1_2011Oct4	ARO-62						0.1238	BE32567	07KNSTD	0.026±0.015	2.1±1.3			
Blank_2_2011Oct4	ARO-63,-66,-67						0.1546	BE32376	07KNSTD	0.027±0.009	2.8±0.9			

Table DR2: Radiocarbon dates on fossil soils within superimposed deposits of the ‘LIA’ composite moraine (Figs. 1 and DR5a,b) and detrital logs found in basal till of the proglacial streambed at Tsidjiore Nouve Glacier (Fig. DR5c) and glacier-climatic significance (Röthlisberger, 1976, Röthlisberger and Schneebeli, 1979). All calibrated ages below are given as 2σ intervals, referenced to the year 1950 CE (=BP, before present). They are calibrated with OxCal 4.1 (Bronk Ramsey, 2009, 2011) relative to the IntCal09 calibration data set (Reimer et al., 2009).

Dated material	Uncal. age (^{14}C -yr)	Cal. age (yr BP)	Glacier-climatic significance
Upper fossil soil in moraine	1075 ± 80	1180-800	Timing of ‘favorable’ (warm) climate, minimum age for moraine deposition
Lower fossil soil in moraine	1380 ± 85	1510-1080	
Fossil log	2940 ± 150	3440-2770	Timing of glacier advance, following a period of warmer climate
Fossil log	8400 ± 200	10120-8780	

Table DR3: Statistics of the ^{10}Be ages from the crest and the recessional ridges of the pre-LIA moraine including different mean ages with respective uncertainties and the reduced chi-squares. For the ‘weighted mean’, both mean age and uncertainty were weighted by the inverse variances (e.g. Taylor, 1997). The relative high chi-square value is a result of the exceptionally small 1σ analytical errors of the individual ages ($\sim 1.5\%$). Hence, for both crest and recessional ridges the boulder age distributions indicate that significant errors due to complex geological conditions (inheritance from prior exposure, erosion, or boulder instability) or snow cover are unlikely.

	^{10}B ages on crest (n=10)	^{10}Be ages on recessional ridges (n=7)
Arithmetic mean \pm standard deviation	11,440 \pm 380 years	11,230 \pm 210 years
- incl. production rate uncertainty	11,440 \pm 680 years	11,230 \pm 590 years
Weighted mean	11,440 \pm 60 years	11,250 \pm 80 years
Peak age	11,470 years	11,190 years
Median age \pm interquartile range	11,430 \pm 730 years	11,230 \pm 290 years
Reduced χ^2	3.9	0.9

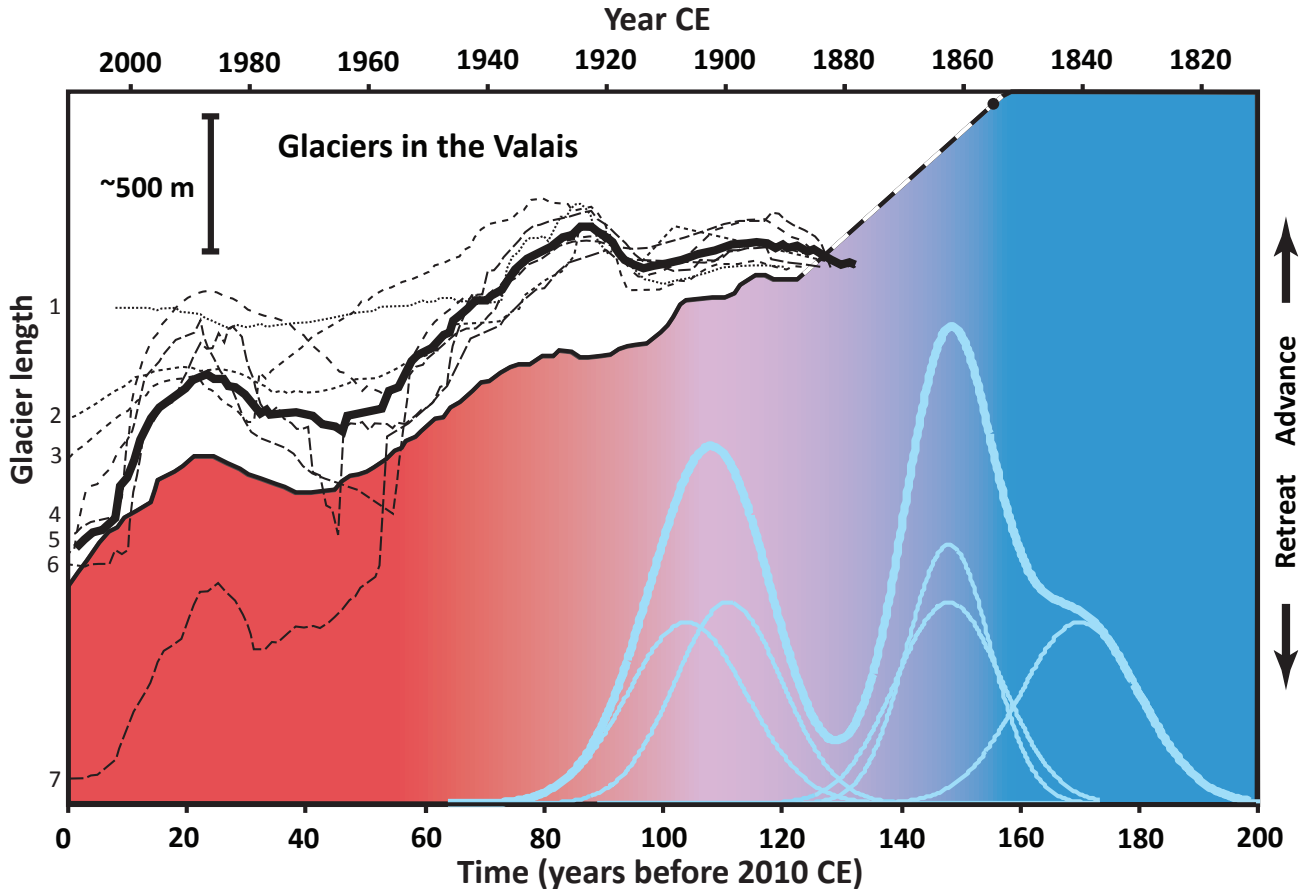


Fig. DR1: Post-LIA length measurements of several glaciers in the Valais, Switzerland. The red and dark blue graph shows length changes of Arolla Glacier (direct neighboring glacier of Tsidjiore Nouve; Glaciological reports, 1881-2009). The dashed thick line of this graph indicates lack of continuous measurements between the years 1856 and 1886. Thin superposed lines are length measurements of seven other glaciers in the Valais starting around the year 1880, with the thick black line representing their average: 1 Fee Glacier, 2 Schwarzberg Glacier, 3 Lang Glacier, 4 Rossbode Glacier, 5 Trient Glacier, 6 Allalin Glacier, 7 Findelen Glacier. All glaciers show similar fluctuation patterns, i.e. during the general retreat from the LIA maximum a two-fold re-advance occurred between 1890 and 1930 CE, followed by another re-advance between 1970 CE and 1990 CE. The thick light blue curve is the summed probability plot of the individual ¹⁰Be ages (thin light blue curves) from the outer post-LIA moraine.



Fig. DR2: Examples of sampled boulders. A and B: ARO-1 (view west) and ARO-59 (view east), respectively, both embedded on the crest of the pre-LIA moraine. C: ARO-16, protruding from a recessional ridge of the pre-LIA moraine, view east.

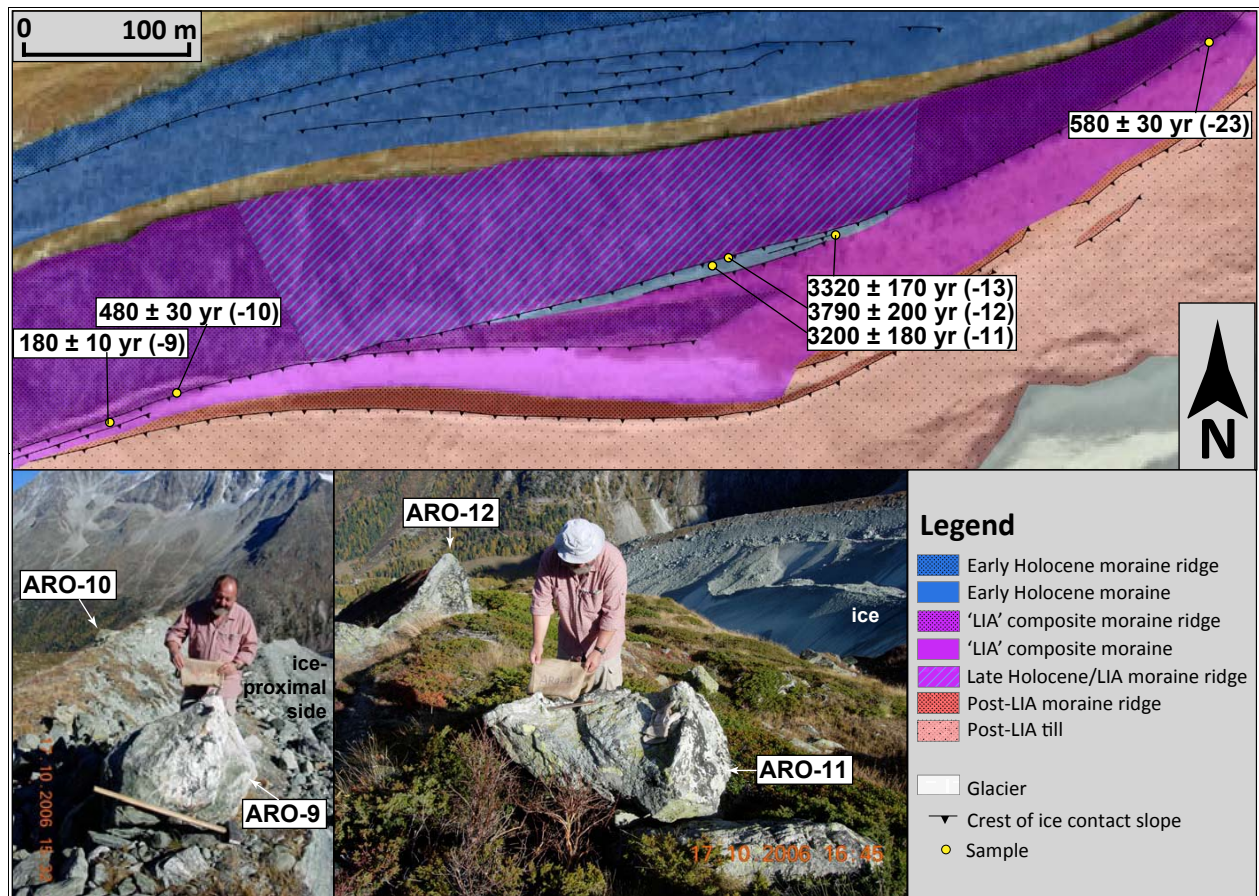


Fig. DR3: Positions of late Holocene and LIA boulders on the 'LIA' composite moraine. The upper panel displays the corresponding sample sites and ages in a zoom-in of the moraine map given in Fig. 1. The left photograph shows the position of boulder ARO-9, which is on a more ice-proximal and thus stratigraphically younger subsection of the composite moraine than boulder ARO-10, in agreement with the ^{10}Be chronology. Similarly, the right picture shows that ARO-12 is in a slightly more ice-distal and therefore stratigraphically older position than ARO-11, again in agreement with the ^{10}Be ages.

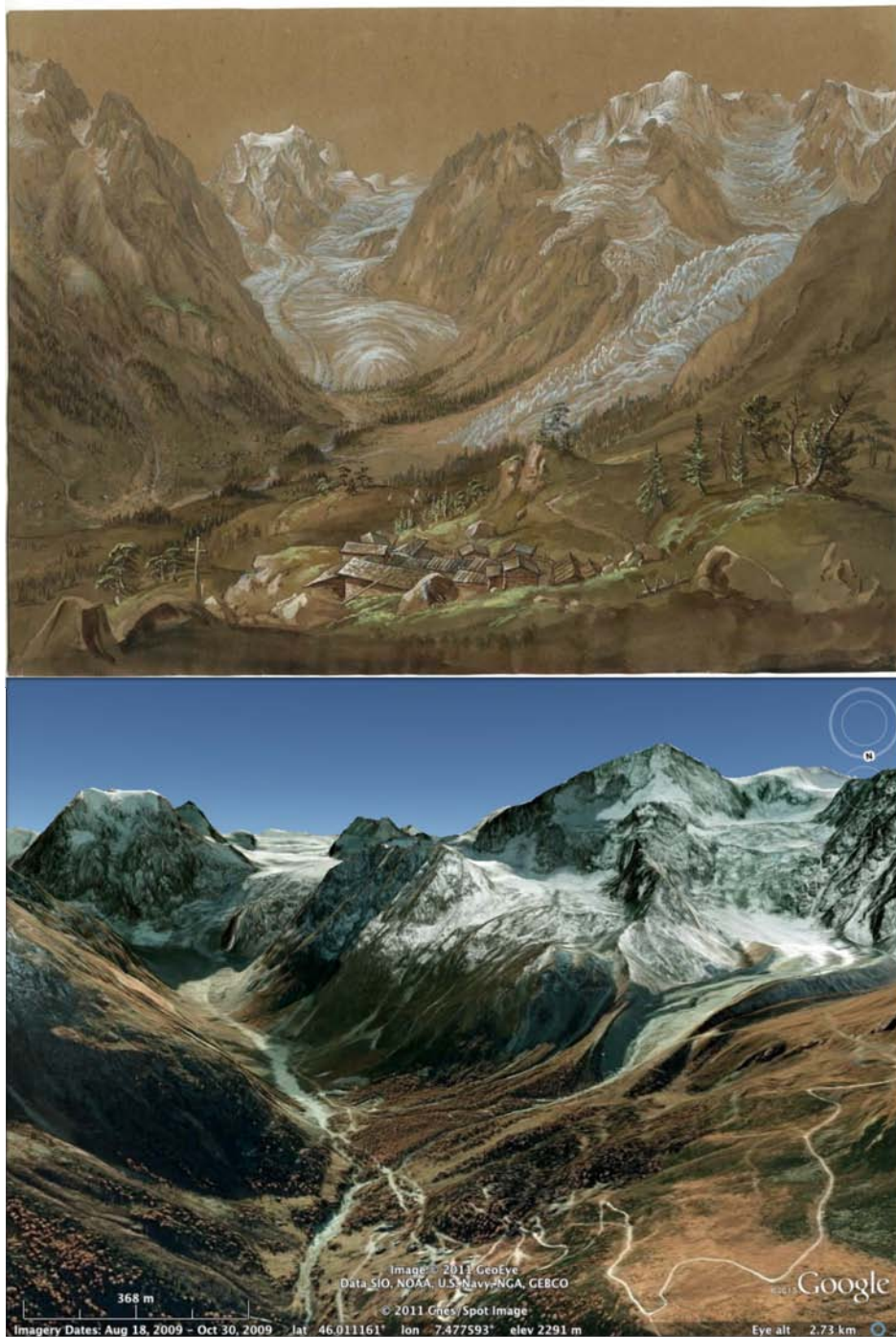


Fig. DR4: Upper panel: Drawing by Bühlmann from the year 1836 CE (Skizzenbücher Bd. 10, 256, Graphische Sammlung ETH, Zürich) showing the Tsidjiore Nouve Glacier on the right, the Arolla Glacier on the left and the village Arolla in the front. Glacier terminus positions are close to their Little Ice Age peak extent. Lower panel: Google Earth picture of approximately the same view in the year 2009 CE.

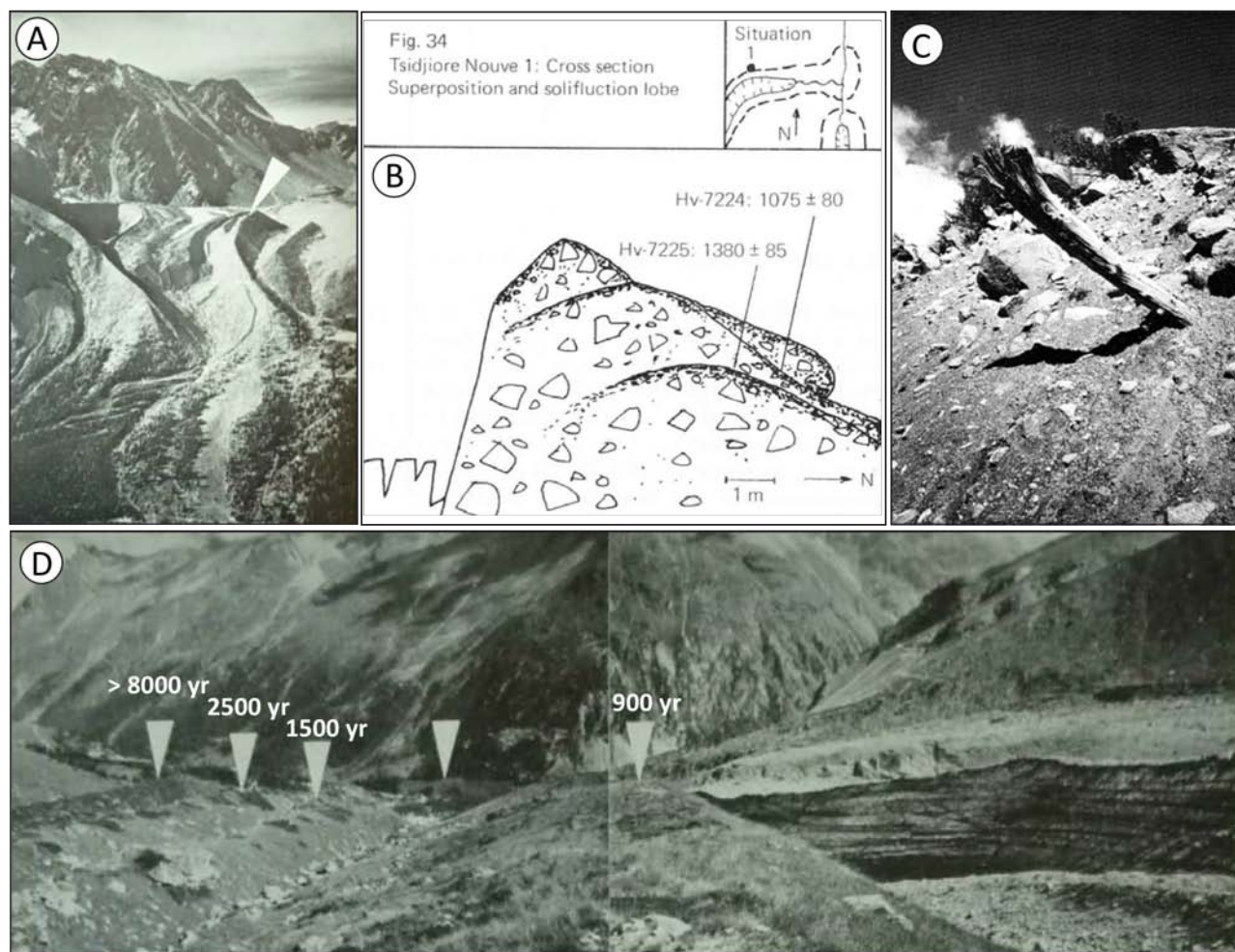


Fig. DR5: Figures from the earlier work on the Holocene moraine sequence at Tsidjiore Nouve Glacier (Röthlisberger, 1976; Röthlisberger and Schneebeli, 1979). A: Photograph of the glacier and the moraine sequence in the year 1972 with white arrow pointing to the location of the excavated fossil soils. B: Schematic illustration of the two fossil soils found in superimposed moraine deposits in the ‘LIA’ composite moraine and corresponding ^{14}C ages. According to the authors, the younger fossil soil was covered by solifluction during a cold period. C: Radiocarbon dated larch log embedded in basal till and washed out by the glacial stream (3440-2770 cal years BP). D: Left lateral moraine sequence with pilot age estimates, which are based on 4 radiocarbon dates at Tsidjiore Nouve Glacier (summary in Table DR2) in combination with radiocarbon dates from the nearby glaciers Findelen, Mont Miné, and Ferpècle (Röthlisberger, 1976; Röthlisberger and Schneebeli, 1979). The deposition ages of 2500, 1500 and 900 years are presumably mostly inferred from ^{14}C ages at the three nearby glaciers. The white arrow in the back points to terminal moraine of the year 1817 CE.

References:

- Balco, G., Stone, J., Lifton, N., and Dunai, T., 2008, A complete and easily accessible means of calculating surface exposure ages or erosion rates from ^{10}Be and ^{26}Al measurements, *Quaternary Geochronology* 3, p. 174-195.
- Balco, G., Briner, J., Finkel, R. C., Rayburn, J. A., Ridge, J. C., and Schaefer, J. M., 2009, Regional beryllium-10 production rate calibration for late-glacial northeastern North America, *Quaternary Geochronology* 4, p. 93-107.
- Bronk Ramsey, C., 2009, Bayesian analysis of radiocarbon dates, *Radiocarbon*, 51, p. 337-360.

Bronk Ramsey, C., 2011. OxCal Program 4.1, http://c14.arch.ox.ac.uk/oxcalhelp/hlp_contents.html

Glaciological reports (1881-2009) "The Swiss Glaciers", Yearbooks of the Cryospheric Commission of the Swiss Academy of Sciences (SCNAT) published since 1964 by the Laboratory of Hydraulics, Hydrology and Glaciology (VAW) of ETH Zürich. No 1-126, (<http://glaciology.ethz.ch/swiss-glaciers/>).

Lal, D., 1991, Cosmic ray labeling of erosion surfaces: in situ nuclide production rates and erosion models, *Earth and Planetary Science Letters* 104, p. 424-439.

Reimer, P.J., and 27 others, 2009, IntCal09 and Marine09 radiocarbon age calibration curves, 0-50,000 years cal BP, *Radiocarbon* 51, p. 1111-1150.

Röthlisberger, F., 1976, Gletscher- und Klimaschwankungen im Raum Zermatt, Ferpècle und Arolla, *Die Alpen* 52, p.59-152.

Röthlisberger, F., and Schneebeli, W., 1979, Genesis of lateral moraine complexes, demonstrated by fossil soils and trunks: indicators of postglacial climatic fluctuations, *in* Schlüchter, C., ed., *Moraines and Varves*. A.A. Balkema, Rotterdam, p. 387-419.

Taylor J.R., 1997, *An Introduction to Error Analysis. The Study of Uncertainties in Physical Measurements*, University Science Books, Sausalito, 327 p.